ACS SyntheticBiology

Letter

pubs.acs.org/synthbio

Engineering Pak1 Allosteric Switches

Onur Dagliyan,[†,‡,§,⊗] Andrei V. Karginov,[∥,⊗] Sho Yagishita,[⊥] Madeline E. Gale,[#] Hui Wang,[‡] Celine DerMardirossian,[▽] Claire M. Wells,[#] Nikolay V. Dokholyan,[†,§] Haruo Kasai,[⊥] and Klaus M. Hahn*[,‡,§]

[†]Department of Biochemistry and Biophysics, [‡]Department of Pharmacology, [§]Lineberger Comprehensive Cancer Center, University of North Carolina at Chapel Hill, Chapel Hill, North Carolina 27599, United States

[∥]Department of Pharmacology, University of Illinois at Chicago, Chicago Illinois 60612, United States

[⊥]Center for Disease Biology and Integrative Medicine, The University of Tokyo, Bunko-ku, Tokyo 113-0033, Japan

[#]Division of Cancer Studies, King's College London, London SE1 1UL, England, U.K.

[▽]Department of Cell and Molecular Biology, Scripps Research Institute, La Jolla, California 92037, United States

Supporting Information

ABSTRACT: P21-activated kinases (PAKs) are important regulators of cell motility and morphology. It has been challenging to interrogate their functions because cells adapt to genetic manipulation of PAK, and because inhibitors act on multiple PAK isoforms. Here we describe genetically encoded PAK1 analogues that can be selectively activated by the membrane-permeable small molecule rapamycin. An engineered domain inserted away from the active site responds to rapamycin to allosterically control activity of the PAK1 isoform. To examine the mechanism of rapamycin-induced PAK1 activation, we used molecular dynamics with graph theory to predict amino acids involved in allosteric communication with the active site. This analysis revealed allosteric pathways that were exploited to generate kinase switches. Activation of PAK1 resulted in transient cell spreading in metastatic breast cancer cells, and long-term dendritic spine enlargement in mouse hippocampal CA1 neurons.

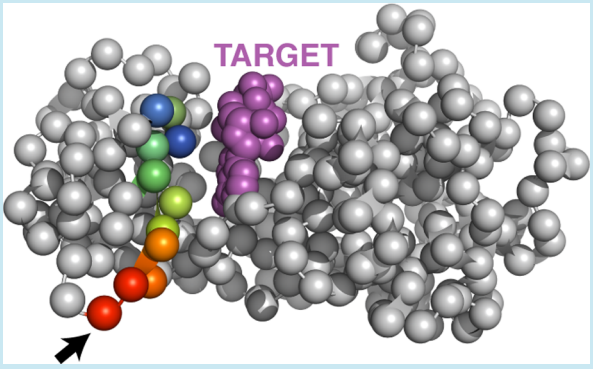

KEYWORDS: *allosteric switch, protein dynamics, PAK, cell motility, dendritic spines*

P21-activated kinases (PAK1−6) are serine/threonine kinases involved in cytoskeletal signaling networks.[1] PAKs have been shown to regulate cell morphodynamics in angiogenesis, synaptic transmission, neurogenesis, and metastasis.[2−5] The role of PAK1 activation kinetics, and the specific roles of different PAK isoforms, remain unclear. PAK inhibitors have been used to probe the roles of PAKs in living systems, but their target specificity is debated.[1]

We previously developed an approach to activate kinases using rapamycin or its nonimmunosuppressive analogues, applied to the Src family kinases Src, Yes and Fyn, to mitogen-activated kinase p38, and to focal adhesion kinase.[6,7] An engineered rapamycin-binding domain was inserted into a surface-exposed loop of the kinase, where its conformational changes were coupled allosterically to the active site. The domain destabilized the ATP binding loop (G-loop) of the kinase, disrupting activity. Rapamycin binding led to restabilization and kinase activation. Here we engineer rapamycin-sensitive switches specifically for the PAK1 isoform, and study the effects of PAK1 activation on cancer cell morphodynamics and hippocampal neuron spine formation. In contrast to the kinases previously targeted,[6−9] PAK is a homodimer in its inactive state.[10] We have identified an additional allosteric site for domain insertion and shed light on the allosteric mechanism used by the engineered domains.

RESULTS AND DISCUSSION

In the present study, we focus on PAK1 because it is the dominant isoform upregulated in human tumors, and it is one of the PAK isoforms expressed in brain. PAK1 consists of a C-terminal kinase domain, and regulatory domains that include a p21-binding domain (PBD) and an inhibitory domain (AI). We produced both dual and single chain PAK1 switches, targeting the kinase domain in both cases (Figure 1A and B). In the dual chain design, we used FK506-binding-protein (FRB) protein together with the insertable FKBP12 domain (iFKBP).[6,7] The iFKBP domain was inserted at an allosteric site within the catalytic domain, causing kinase inactivation. Addition of rapamycin induced binding between the kinase-iFKBP chimera and coexpressed FRB, resulting in stabilization and reactivation of the kinase. This design was named rapamycin-regulated

Received: November 30, 2016
Published: April 3, 2017

DOI: 10.1021/acssynbio.6b00359
ACS Synth. Biol. 2017, 6, 1257−1262

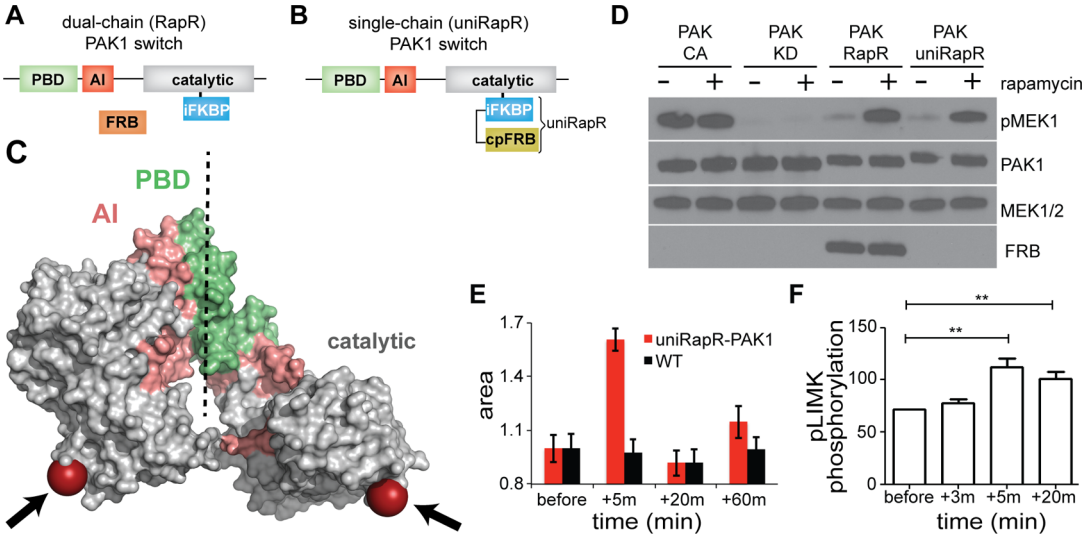

Figure 1. Engineering rapamycin-responsive PAK1 analogues. (A) The dual chain (RapR) PAK1 analogue was built by inserting iFKBP into the catalytic domain. FRB was coexpressed with iFKBP-PAK1. (B) The single chain (uniRapR) PAK1 analogue was built by inserting the uniRapR domain into the catalytic domain as in (a). This system does not require the coexpression of FRB. (C) Crystal structure of PAK1 in the inactive state (PDB id: 1f3m). The autoinhibitory domain (AI) and p21 binding domain (PBD) are shown in salmon and green. Insertion sites are red residues shown with black arrows. (D) Rapamycin-dependent activity of constitutively active (CA) PAK1, kinase-dead (KD) PAK1, RapR-PAK1, and uniRapR-PAK1, shown by monitoring the phosphorylation state of MEK. (E) Area of MDA-MB-231 cells (red) that stably express uniRapR-PAK1 before and after addition of rapamycin. Black denotes cells (WT) that do not express uniRapR-PAK1. (F) Phosphorylation of LIMK in the same cells before and after addition of rapamycin. Error bars represent SEM (n = 3) from three independent experiments. **p < 0.05.

PAK1 (RapR PAK1, Figure 1A). In the single chain or unimolecular (uniRapR) design, a single domain combining iFKBP and FRB was inserted at the allosteric site; this similarly conferred rapamycin regulated activity (Figure 1B). The dual-chain design is advantageous in that it can be used to cause activated PAK1 to interact with specific target molecules.[9] The single-chain design is more convenient for simple PAK1 activation and does not show heterogeneous responses stemming from varied expression ratios of the two chains.[7] The insertion site previously used successfully for other kinases was tested first. This site is not evolutionary conserved (Figure S1), and does not interact with the regulatory domain, the dimerization interface (Figure 1C), or any other structural elements in the protein (Figure S2). These characteristics led us to choose the 288−293 PAK1 loop for insertion of the engineered domains.

In order to increase kinase activity upon activation, and to remove any PAK1 regulation other than simple rapamycin-induced activation, we introduced phospho-mimetic S422D/T423E mutations into PAK1 to render it constitutively active. Our previous work showed that flexible linkers between the rapamycin sensitive domain and the host protein enable folding of the two domains, but reduce effective allosteric transmission from the sensory domain to the host protein. Conversely, short linkers increase the efficiency of allosteric transmission, but can restrain proper folding of two domains.[6−8,11] Considering these criteria, we tested several linkers between the rapamycin sensitive domain and the kinase domain. For the dual chain analogue, four variants of engineered PAK1 were prepared: (1) iFKBP replacing Ala291 and connected Gly-Pro-Gly linkers on both sides; (2−3) iFKBP replacing the Asp289-Gly293 residues and connected using either Gly or Gly-Pro-Gly linkers; (4) iFKBP replacing Met288-Gln294 residues and connected *via* Gly-Pro-Gly linkers. We coexpressed each construct with FRB in HEK293T cells and, following immunoprecipitation of PAK1, tested kinase activity using a PAK1 substrate, MEK1, which is phosphorylated at residue S298.[12] Replacement of Asp289-Gly293 with iFKBP flanked by GPG linkers produced optimal rapamycin regulation of engineered PAK1 (Figure S3). We named this optimized version rapamycin-regulatable PAK1 (RapR-PAK1). FRB was present in the pull-down samples, showing binding of FRB to PAK1-iFKBP. In control experiments, constitutively active PAK1 alone did not respond to rapamycin, and kinase-dead PAK1 alone was inactive in the absence or presence of rapamycin (Figure S3). These experiments demonstrated that insertion of the iFKBP domain into the loop between residues 288 and 293 generated a robust, regulatable dual chain PAK1 analogue. We next made a single chain rapamycin-responsive PAK1 by replacing iFKBP with the uniRapR domain. To increase the dynamic range of uniRapR-PAK1, we introduced a mutation (L107F) on the interface that enhanced PAK1 activity (Figure S3).[13] We directly compared the dual chain RapR-PAK1 with the single chain uniRapR-PAK1 by monitoring the phosphorylation of endogenous MEK1 upon addition of rapamycin into the cell medium. Similar to RapR-PAK1, uniRapR-PAK1 was inactive without rapamycin and was activated by rapamycin (Figure 1D). *In vitro* kinase assays demonstrated regulation of UniRapR-PAK1 by rapamycin (Figure S3). These results showed that both the dual and single chain PAK1 analogues could be efficiently activated in living cells by rapamycin.

PAK1 has been identified as an oncogene that transforms breast epithelial cells,[14] and overexpression of mutant PAK1 increases the migration rates of breast cancer cells.[15] To test the effects of PAK1 kinase activity on breast cancer cell morphodynamics, we expressed uniRapR-PAK1 in the metastatic basal B triple-negative breast cancer cell line MDA-MB-231 and measured the area of cells 5, 20, and 60 min after rapamycin addition. The cells showed an increase in area within 5 min of Pak1 activation (Figure 1E) but later returned to their original morphology within 20 min. Previous studies suggested that LIM kinase 1 (LIMK1), a substrate of

DOI: 10.1021/acssynbio.6b00359
ACS Synth. Biol. 2017, 6, 1257−1262

PAKs, might contribute to the invasive behavior of breast cancer cells.[16] Consistent with this hypothesis, phosphorylation of LIMK was also maximized at the 5 min time point and decreased at the 20 min time point (Figure 1F). Control cells exhibited no response to rapamycin. These results demonstrate the ability of RapR PAK1 to control cell morphology, support a role for the PAK1 isoform in motility and metastasis, and indicate that PAK1 activity alone is not sufficient to induce cell polarization and motility.

PAK1 has been shown to be involved in neuronal spine morphology, synaptic transmission, and pathological conditions including mental retardation and schizophrenia.[17] The kinase activity of PAK is important in brain physiology, because PAK inhibitors have been shown to ameliorate schizophrenia-associated dendritic spine deterioration.[18] It remains unclear which isoform is responsible for these effects. We previously showed that *in vivo* activation of Rac1, an activator of PAK, leads to spine shrinkage in the neocortex.[19] We therefore asked how acute rapamycin-regulatable activation of PAK1 leads to the morphological changes of dendritic spines in the hippocampus. We expressed RapR-PAK1-EGFP in hippocampal CA1 neurons (Figure 2A), and observed that activation of PAK1 led

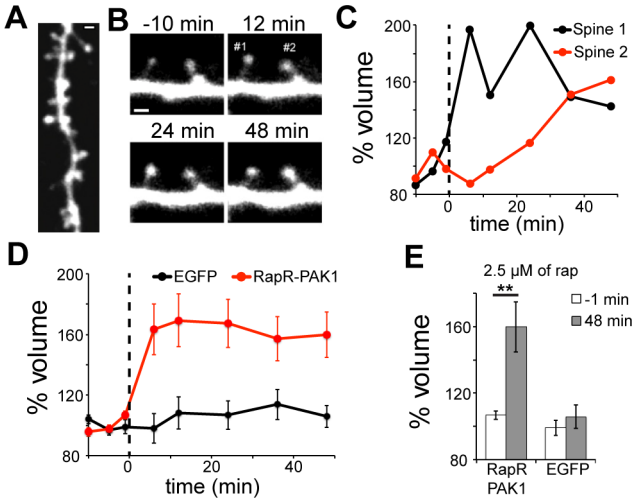

Figure 2. Enlargement of dendritic spines induced by rapamycin. (A) Image of RapR-PAK1-Venus in a dendrite. (B) A series of RapR-PAK1-Venus images in a dendrite before and after stimulation with rapamycin (2.5 μM), which was applied in the period between 0 and 15 min. (C) Volume changes of two spines (#1 and #2) indicated in (B). The changes were estimated from the total fluorescence of RapR-PAK1-Venus in the spines. (D) Mean time courses of spine volume obtained from 33 or 13 spines in either RapR-PAK1-Venus or EGFP along with FRB-mCherry transfected neurons. Error bars indicate SEM. (E) Statistical comparisons of the effects of rapamycin (2.5 μM) shown in (D). *$p < 0.05$, **$p < 0.01$. Scale bars indicate μm.

to long-term dendritic spine enlargement (>40 min) (Figure 2B). Although each spine responded to rapamycin with different kinetics (Figure 2C), there was an overall persistent increase in the spine volume (area of change 60% ± 15%, n = 35 spines), whereas neurons expressing only EGFP did not respond to rapamycin (n = 13 spines) (Figure 2D and E). Based on these results, we concluded that acute activation of PAK1 leads to long-term dendritic spine enlargement, suggesting insights into the roles of the PAK1 isoform in long-term-potentiation, learning and memory.

Our previous molecular dynamic modeling of focal adhesion kinase showed that the iFKBP insertion loop moves in concert with the kinase G-loop.[6] We hypothesized that residues which move in concert are allosterically coupled, so loops that move in concert with the active site are good candidates for insertion of an allosteric control domain. To test this hypothesis, we analyzed PAK1 kinase domain using discrete molecular dynamics.[20,21] In Figure 3A, the correlation coefficients for the motions of each α carbon pair are represented as a heat map, showing that motions of the iFKBP insertion loop (L1) correlate with those of the catalytic site, particularly with the ATP binding G-loop. This analysis also revealed another loop (L2) whose motions correlated with those of the ATP binding site. Similar to L1, this loop is solvent exposed and is not evolutionarily conserved (Figure S4). To test whether insertion of the uniRapR domain into the L2 loop produces an allosteric switch, we substituted residues G337 and D338 in L2 with the uniRapR domain. Similar to the original PAK1 analogue (uniRapR-PAK1-L1), the uniRapR-PAK1-L2 analogue responded to rapamycin (Figure 3B). We reduced the slight off-state activity by removing two residues from the loop, V336 and E339 (Figure 3B). These results, along with linker optimization of the first analogue (Figure S3), showed that on/off state activity can be adjusted through linker optimization (Figure 3B). For PAK1, shortening the loop or removing residues from the insertion loop reduced off state activity, and on state activity was increased by elongating the loop using flexible residues. We also inserted the uniRapR domain into two additional loops (L3 and L4). Like L1 and L2, L3 connects two β-strands that interact with ATP, and its motion correlates with the motions of ATP binding sites (Figure S5). In contrast, L4 is in the flexible linker connecting two lobes of the kinase. Biochemical assays showed that insertion of uniRapR into L3 generated rapamycin-dependent PAK1 activity, whereas the PAK1 analogue produced by inserting uniRapR into L4 was not affected by insertion or rapamycin. This data showed that a PAK1 switch could be generated by inserting uniRapR into loops whose motions correlated with the motions of the catalytic site.

We hypothesized that the inserted allosteric switch affected the active site because changes in switch movement affected active site movement. Residues that move in concert throughout the kinase domain may constitute an allosteric path to propagate changes between engineered domains and the active site. To track such propagation pathways, we used a graph theory, converting motion dynamics of residues into an undirected network in which nodes represent residues, edges represent contacts, and edge weights are correlation coefficients (Figure 3B). The shortest path from insertion loops L1 or L2 to the catalytic site was calculated using Dijkstra's algorithm (Figure 3C),[22] indicating that the propagation from L1 is transmitted through the strands located between residues G293-Q300 and G282-D289 (Figure 3D). Interestingly, such intrastrand propagation is not present in the case of L2, where the perturbation is propagated in an interstrand manner between strands E339-E345, G293-N302, D282-D289, and E274-D289 (Figure 3D and E). As an alternative approach, we analyzed potential allosteric pathways using coevolution of residues,[23] as previously described.[24] Prediction of residues that coevolve with the catalytic site indicated a similar interstrand pathway (Figure S6). Correlated motions in ß-sheets have been suggested to be fundamental for allosteric regulation of protein function.[25] Together these results showed that perturbation is

DOI: 10.1021/acssynbio.6b00359
ACS Synth. Biol. 2017, 6, 1257−1262

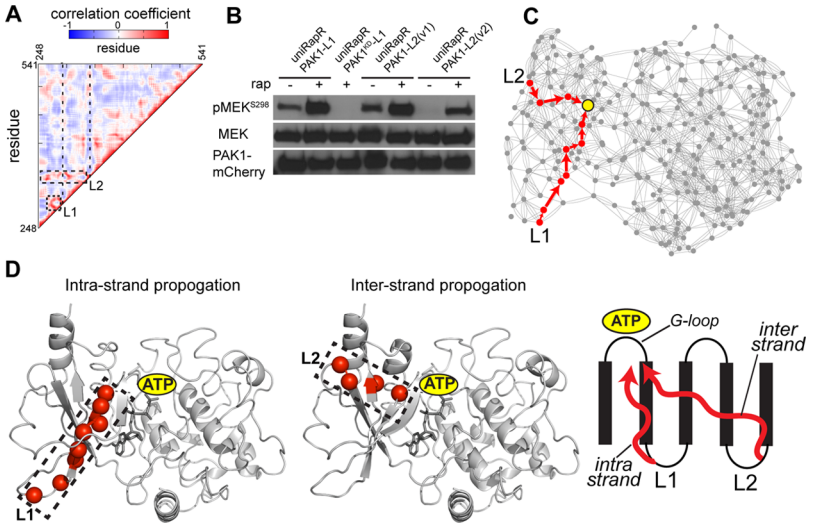

Figure 3. Understanding the mechanism of allosteric propagation to generate PAK1 analogues. (A) Correlative motions of residues in the PAK1 kinase domain, computed by discrete molecular dynamics. Red and blue denote correlation and anticorrelation between two residues, respectively. (B) Insertion of uniRapR into both identified insertion sites conferred control by rapamycin. In the second version of the L2-based analogue (uniRapR-PAK1-L2-v2), the loop residues from PAK1 were removed, resulting in tighter control. (C) Network representation of the kinase domain based on residue−residue contacts (<5.5A). Gray nodes represent residues; edges represent the contacts between α-carbons. L1 and L2 insertion sites are shown. Red arrows represent the propagation pathways from the insertion loop to the ATP binding site (yellow node). (D) Suggested mechanism of PAK1 switching generated using L1 loop (left) and L2 loop (middle). Illustration of the mechanisms of PAK1 analogues (right). The perturbation is transmitted from L1 and L2 to the G-loop through intra-and interstrand pathways, respectively.

propagated from our two insertion loops (L1 and L2) *via* intrastrand and interstrand pathways, respectively. This notion will be helpful for generation of new kinase switches, and for application to other protein families.[11,23,26]

EXPERIMENTAL PROCEDURES

DNA Constructs. All restriction enzymes were purchased from New England Biolabs. pmVenus-N1-PAK1 was a gift from Jonathan Chernoff. Point mutations and insertions of iFKBP and uniRapR sequences into PAK1 were done with the Quikchange mutagenesis kit (Stratagene). Retroviral plasmids were generated by cloning uniRapR-PAK1-mCherry into pBABE-Tet-Off-puro plasmid (Clontech).

Biochemical Characterization of the Kinase Activity. Cell transfection, immunoprecipitation, and testing kinase activity were performed as described previously.[7] See Supplemental Experimental Procedures for details. HEK293 cells were transfected with 1 μg of DNA constructs using Fugene 6 reagent (Roche) using manufacturer's guidelines. After 24 h of transfection, cells were treated with either rapamycin (Sigma) or an equivalent volume of ethanol for 30 min. Cells were lysed with lysis buffer (50 mM Tris pH 7.4, 150 mM NaCl, 1% Triton X-100 and Roche protease inhibitor cocktail). Endogenous phosphorylation of MEK was detected by Western blotting. For immunoprecipitation experiments, cleared lysates were incubated with protein-G beads attached to anti-GFP antibody (JL8, Clontech) for 2 h. The beads were washed three times with lysis buffer, and then with kinase buffer (2 mM Tris, pH 8.0, 10 mM $MgCl_2$) for phosphorylation assays. 800 ng purified MEK, ATP (100 μM) in 40 μL of kinase buffer containing 1 μM of dTT were mixed with bead suspension for 10 min at 30 °C. Reactions were quenched by adding sample loading buffer and boiling for 5 min. Phosphorylated MEK was detected in pull-down samples by Western blotting using anti-pMEK-S298 and anti-MEK1/2 antibodies (Cell Signaling).

Imaging of MDA-MB-231 Cells. After 2 days without doxcyline, cells were seeded at 10,000 cells per well in DMEM with puromycin on fibronectin coated coverslips (10 μg/mL). The next morning (about 6 h before the experiment), cell media was replaced with DMEM (2% FBS), with 450 μL in each well of a 4 well plate. Cells were incubated with 500 nM rapamycin for 5, 20, and 60 min. Cells were then fixed in 4% PFA (in PBS) and stained with DAPI (1:10 000) and phalloidin Alexa488 (1:1000). Cells were imaged with an Olympus IX71 inverted microscope.

Imaging of Mouse Hippocampal Cells. Hippocampal slices with a thickness of 350 μm were prepared from 7-day-old Sprague−Dawley rats. Slices were mounted on 0.4-μm culture inserts (Millipore, Billerica, MA) and incubated at 35 °C under 5% CO_2 in a medium consisting of 50% MEM (Invitrogen, Carlsbad, CA), 25% Hanks' balanced salt solution (Invitrogen), 25% horse serum (Nichirei, Tokyo, Japan), and glucose (6.5 g/L) (Nacalai Tesque, Kyoto, Japan). After 4 days in culture, the slices were transfected with a Gene Gun system (PDS-1000; Bio-Rad, Hercules, CA) with RapR-PAK-Venus and FRB-mCherry. Imaging experiments were performed 3 days after the transfection. Each culture insert was transferred to a recording chamber and superfused with a solution (ACSF) that contained 125 mM NaCl, 2.5 mM KCl, 2 mM $CaCl_2$, 1 mM $MgCl_2$,1.25 mM NaH_2PO_4, 26 mM $NaHCO_3$, 20 mM glucose, 1uM TTX, and 200uM Trolox, and had been equilibrated with 95% O_2 and 5% CO_2. Rapamycin (Wako, Tokyo) was applied through bath perfusion. All physiological experiments were performed at room temperature (23° to 25 °C). The experiments were approved by the Animal Experiment Committee of the Faculty of Medicine, University of Tokyo. Two-photon imaging of dendritic spines was performed with an upright microscope (BX61WI; Olympus, Tokyo, Japan) equipped with a FV1000 laser-scanning microscope system (FV1000, Olympus) and a water-immersion objective lens (LUMPLFLN60xW, numerical aperture 0.9). We use a mode-locked, femtosecond-pulse

DOI: 10.1021/acssynbio.6b00359
ACS Synth. Biol. 2017, 6, 1257−1262

Ti:sapphire lasers (MaiTai from Spectra Physics, Mountain View, CA; Chameleon from Coherent, Santa Clara, CA) with a wavelength of 970 nm. Emitted fluorescence was acquired at 488 to 560 nm and 590 to 680 nm for Venus and mCherry, respectively. Three-dimensional reconstructions of dendritic morphology were generated by the summation of Venus fluorescence values separated by 0.5 μm. The spine-head volumes were estimated from the total fluorescent intensity.

Molecular Modeling, Discrete Molecular Dynamics, and Correlative Motion Analysis. The crystal structure of the kinase domain was obtained from the Protein data bank (PDB id: 1f3m), and Medusa Toolkit was used to model the protein.[27] All simulations were performed using all-atom discrete molecular dynamics.[20,28] Atomic clashes were corrected and the protein was minimized at heat exchange coefficient 10 at 0.7 kcal/mol·k_B with a harmonic potential constant of 1 kcal/mol·A^2. The system was then packed at 0.3 kcal/mol·k_B with heat exchange coefficient 1. Upon packing, the system was simulated at 0.4 kcal/mol·k_B for 1 million DMD steps.[29] Cα represent nodes of the graph, edges represent the connection between nodes. Edge weight is based on the correlation coefficient calculated by correlative motion analysis. The shortest distance between two selected residues were calculated by Dijkstra's algorithm.[22]

Sequence Conservation and Coevolution Analysis. Pfam was used to obtain protein kinase domain sequences.[30] The MISTIC server was used to calculate sequence conservation and coevolving mutual information.[24]

■ ASSOCIATED CONTENT

Supporting Information

The Supporting Information is available free of charge on the ACS Publications website at DOI: 10.1021/acssynbio.6b00359.

Figures S1−S6; Pak structures showing important domains, sites of insertion, and their properties; Assays showing control of kinase activity with insertion at different sites; Coevolved residues in the kinase domain (PDF)

■ AUTHOR INFORMATION

Corresponding Author

*E-mail: khahn@med.unc.edu.

ORCID

Onur Dagliyan: 0000-0003-1825-1011

Author Contributions

⊗O.D. and A.V.K. are co-first authors. O.D., A.V.K., and K.M.H. carried out and designed all research not otherwise attributed. S.Y. and H.K. performed and interpreted neuronal imaging, M.E.G. and C.M.W. carried out and interpreted MDA-MB-231 cell experiments. N.V.D. was responsible for the computational aspect of the project. C.D. contributed to analysis. H.W. contributed to the characterization of uniRapR-PAK1. O.D. and K.M.H. wrote the manuscript with input from all authors.

Notes

The authors declare no competing financial interest.

■ ACKNOWLEDGMENTS

O.D. is an HHMI International Student Research Fellow. This work was supported by NIH grants R01CA175747 and P41-EB002025 (K.M.H), NIH R01GM080742 (N.V.D), a Grant-in-Aid for Scientific Research (S) No. 26221001 from the Japanese Ministry of Education, Culture, Sports, Science, and Technology (H.K.), the CREST program (JPMJCR1652 to H.K.) of the Japan Science and Technology Agency (H.K, J.S.T.), and the Human Frontiers in Science Program (K.M.H. and H.K.).

■ REFERENCES

(1) Radu, M., Semenova, G., Kosoff, R., and Chernoff, J. (2014) PAK signalling during the development and progression of cancer. *Nat. Rev. Cancer 14*, 13−25.

(2) Hofmann, C., Shepelev, M., and Chernoff, J. (2004) The genetics of Pak. *J. Cell Sci. 117*, 4343−4354.

(3) Dan, C., Nath, N., Liberto, M., and Minden, A. (2002) PAK5, a new brain-specific kinase, promotes neurite outgrowth in N1E-115 cells. *Mol. Cell. Biol. 22*, 567−577.

(4) Zhang, H., Webb, D. J., Asmussen, H., Niu, S., and Horwitz, A. F. (2005) A GIT1/PIX/Rac/PAK signaling module regulates spine morphogenesis and synapse formation through MLC. *J. Neurosci. 25*, 3379−3388.

(5) Allen, K. M., Gleeson, J. G., Bagrodia, S., Partington, M. W., MacMillan, J. C., Cerione, R. A., Mulley, J. C., and Walsh, C. A. (1998) PAK3 mutation in nonsyndromic X-linked mental retardation. *Nat. Genet. 20*, 25−30.

(6) Karginov, A. V., Ding, F., Kota, P., Dokholyan, N. V., and Hahn, K. M. (2010) Engineered allosteric activation of kinases in living cells. *Nat. Biotechnol. 28*, 743−747.

(7) Dagliyan, O., Shirvanyants, D., Karginov, A. V., Ding, F., Fee, L., Chandrasekaran, S. N., Freisinger, C. M., Smolen, G. A., Huttenlocher, A., Hahn, K. M., and Dokholyan, N. V. (2013) Rational design of a ligand-controlled protein conformational switch. *Proc. Natl. Acad. Sci. U. S. A. 110*, 6800−6804.

(8) Chu, P. H., Tsygankov, D., Berginski, M. E., Dagliyan, O., Gomez, S. M., Elston, T. C., Karginov, A. V., and Hahn, K. M. (2014) Engineered kinase activation reveals unique morphodynamic phenotypes and associated trafficking for Src family isoforms. *Proc. Natl. Acad. Sci. U. S. A. 111*, 12420−12425.

(9) Karginov, A. V., Tsygankov, D., Berginski, M., Chu, P. H., Trudeau, E. D., Yi, J. J., Gomez, S., Elston, T. C., and Hahn, K. M. (2014) Dissecting motility signaling through activation of specific Src-effector complexes. *Nat. Chem. Biol. 10*, 286−290.

(10) Lei, M., Lu, W., Meng, W., Parrini, M. C., Eck, M. J., Mayer, B. J., and Harrison, S. C. (2000) Structure of PAK1 in an autoinhibited conformation reveals a multistage activation switch. *Cell 102*, 387−397.

(11) Dagliyan, O., Tarnawski, M., Chu, P. H., Shirvanyants, D., Schlichting, I., Dokholyan, N. V., and Hahn, K. M. (2016) Engineering extrinsic disorder to control protein activity in living cells. *Science 354*, 1441−1444.

(12) Frost, J. A., Khokhlatchev, A., Stippec, S., White, M. A., and Cobb, M. H. (1998) Differential effects of PAK1-activating mutations reveal activity-dependent and -independent effects on cytoskeletal regulation. *J. Biol. Chem. 273*, 28191−28198.

(13) Brown, J. L., Stowers, L., Baer, M., Trejo, J., Coughlin, S., and Chant, J. (1996) Human Ste20 homologue hPAK1 links GTPases to the JNK MAP kinase pathway. *Curr. Biol. 6*, 598−605.

(14) Shrestha, Y., Schafer, E. J., Boehm, J. S., Thomas, S. R., He, F., Du, J., Wang, S., Barretina, J., Weir, B. A., Zhao, J. J., Polyak, K., Golub, T. R., Beroukhim, R., and Hahn, W. C. (2012) PAK1 is a breast cancer oncogene that coordinately activates MAPK and MET signaling. *Oncogene 31*, 3397−3408.

(15) Hammer, A., Rider, L., Oladimeji, P., Cook, L., Li, Q., Mattingly, R. R., and Diakonova, M. (2013) Tyrosyl phosphorylated PAK1 regulates breast cancer cell motility in response to prolactin through filamin A. *Mol. Endocrinol. 27*, 455−465.

(16) Yoshioka, K., Foletta, V., Bernard, O., and Itoh, K. (2003) A role for LIM kinase in cancer invasion. *Proc. Natl. Acad. Sci. U. S. A. 100*, 7247−7252.

DOI: 10.1021/acssynbio.6b00359
ACS Synth. Biol. 2017, 6, 1257−1262

(17) Kreis, P., and Barnier, J. V. (2009) PAK signalling in neuronal physiology. *Cell. Signalling 21*, 384−393.
(18) Hayashi-Takagi, A., Araki, Y., Nakamura, M., Vollrath, B., Duron, S. G., Yan, Z., Kasai, H., Huganir, R. L., Campbell, D. A., and Sawa, A. (2014) PAKs inhibitors ameliorate schizophrenia-associated dendritic spine deterioration in vitro and in vivo during late adolescence. *Proc. Natl. Acad. Sci. U. S. A. 111*, 6461−6466.
(19) Hayashi-Takagi, A., Yagishita, S., Nakamura, M., Shirai, F., Wu, Y. I., Loshbaugh, A. L., Kuhlman, B., Hahn, K. M., and Kasai, H. (2015) Labelling and optical erasure of synaptic memory traces in the motor cortex. *Nature 525*, 333−338.
(20) Ding, F., Tsao, D., Nie, H., and Dokholyan, N. V. (2008) Ab initio folding of proteins with all-atom discrete molecular dynamics. *Structure 16*, 1010−1018.
(21) Dagliyan, O., Proctor, E. A., D'Auria, K. M., Ding, F., and Dokholyan, N. V. (2011) Structural and dynamic determinants of protein-peptide recognition. *Structure 19*, 1837−1845.
(22) Dijkstra, E. W. (1959) A note on two problems in connexion with graphs. *Numer. Math. 1*, 269−271.
(23) Lee, J., Natarajan, M., Nashine, V. C., Socolich, M., Vo, T., Russ, W. P., Benkovic, S. J., and Ranganathan, R. (2008) Surface sites for engineering allosteric control in proteins. *Science 322*, 438−442.
(24) Simonetti, F. L., Teppa, E., Chernomoretz, A., Nielsen, M., and Marino Buslje, C. (2013) MISTIC: Mutual information server to infer coevolution. *Nucleic Acids Res. 41*, W8−14.
(25) Fenwick, R. B., Orellana, L., Esteban-Martin, S., Orozco, M., and Salvatella, X. (2014) Correlated motions are a fundamental property of beta-sheets. *Nat. Commun. 5*, 4070.
(26) Reynolds, K. A., McLaughlin, R. N., and Ranganathan, R. (2011) Hot spots for allosteric regulation on protein surfaces. *Cell 147*, 1564−1575.
(27) Yin, S., Ding, F., and Dokholyan, N. V. (2007) Eris: an automated estimator of protein stability. *Nat. Methods 4*, 466−467.
(28) Zhou, Y., and Karplus, M. (1999) Interpreting the folding kinetics of helical proteins. *Nature 401*, 400−403.
(29) Shirvanyants, D., Ding, F., Tsao, D., Ramachandran, S., and Dokholyan, N. V. (2012) Discrete molecular dynamics: an efficient and versatile simulation method for fine protein characterization. *J. Phys. Chem. B 116*, 8375−8382.
(30) Finn, R. D., Bateman, A., Clements, J., Coggill, P., Eberhardt, R. Y., Eddy, S. R., Heger, A., Hetherington, K., Holm, L., Mistry, J., Sonnhammer, E. L., Tate, J., and Punta, M. (2014) Pfam: the protein families database. *Nucleic Acids Res. 42*, D222−230.

DOI: 10.1021/acssynbio.6b00359
ACS Synth. Biol. 2017, 6, 1257−1262